Photovoltaics

DOI: 10.1002/anie.201303216

Photovoltaic Wire with High Efficiency Attached onto and Detached from a Substrate Using a Magnetic Field**

*Hao Sun, Zhibin Yang, Xuli Chen, Longbin Qiu, Xiao You, Peining Chen, and Huisheng Peng**

Portable electronic equipment represents a mainstream direction in the future.[1,2] To this end, it is critically important to develop portable energy systems such as photovoltaic devices which should be lightweight and can be easily fabricated and operated with high performance. Unfortunately, for either silicon-based, dye-sensitized or polymeric photovoltaic devices, they generally appear in a heavy plate, which could not effectively meet the above requirement.[2–5] In particular, for the use in many portable electronic facilities such as spacecraft, the photovoltaic devices are further required to be able to be removed remotely as a physical detachment is not allowed or available,[6] though it remains unavailable yet. Recently, some attempts were made to explore solar cells in a wire format which showed unique advantages such as a light weight compared with the conventional planar structure.[5d] The wires can also be interwoven. These photovoltaic wires shed light on the development of portable electronic equipment. However, they are not responsive to environmental stimuli and cannot be remotely controlled. In addition, the wire-shaped solar cells also suffer from much lower energy conversion efficiencies than their planar counterparts.

To fabricate the novel solar cell which may be fixed onto and detached from the electronic equipment remotely, a possible solution is to integrate new responsive functionalities, for example, they can be remotely operated by external forces such as magnetic fields. The superparamagnetic properties of many metal oxide and metal nanoparticles have been widely studied in recent years and represent ideal candidates to meet this requirement.[7] Herein, we have developed a new family of dye-sensitized photovoltaic wires where superparamagnetic metal oxide and metal nanoparticles are incorporated into electrodes. These photovoltaic wires can be easily attached onto a substrate using a magnetic field during their use and then removed from the substrate after their use. These new photovoltaic wires have also exhibited a record energy conversion efficiency of 8.03% in wire-shaped devices.[5d] The combined advantages of such wire-shaped solar cells are promising to various portable and wearable electronic applications.[8]

The photovoltaic wire with magnetic response and high efficiency was realized by designing and synthesizing a series of nanostructured materials including carbon nanotubes (CNT), superparamagnetic nanoparticles, and TiO_2 nanotubes. Figure 1 a schematically shows the structure of a typical photovoltaic wire where a CNT composite fiber incorporating superparamagnetic nanoparticles was twisted with a Ti wire grown with TiO_2 nanotubes on the surface. Here the composite fiber served as a counter electrode, while the modified Ti wire functioned as the working electrode.

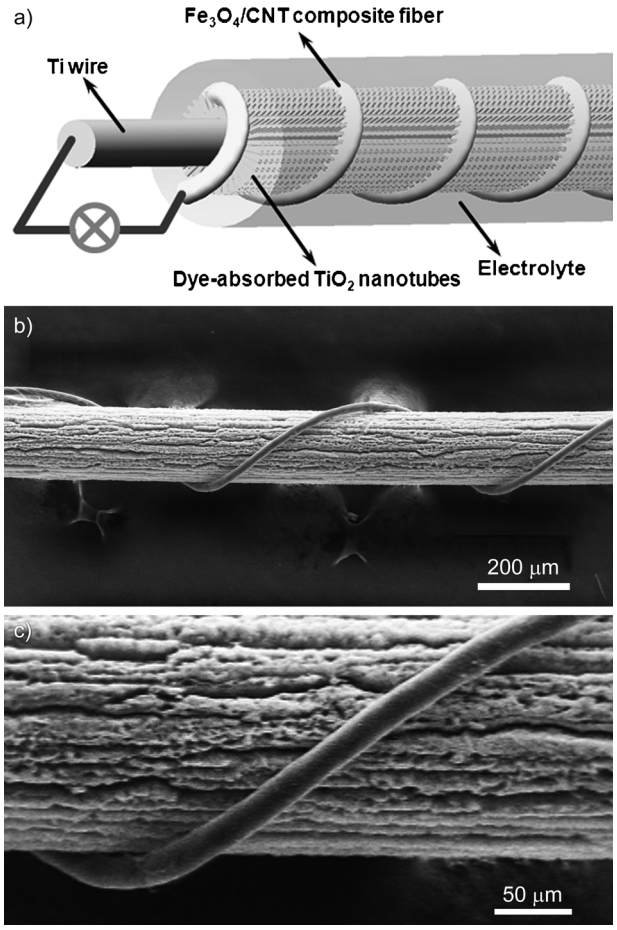

Figure 1. Photovoltaic wire by twisting a TiO_2 nanotube-modified titanium wire which serves as a working electrode and an Fe_3O_4/CNT composite fiber which functions as the counter electrode together. a) Schematic illustration. b) SEM image. c) Higher magnification of (b).

[*] H. Sun, Z. Yang, X. Chen, L. Qiu, X. You, P. Chen, Prof. H. Peng
State Key Laboratory of Molecular Engineering of Polymers
Department of Macromolecular Science and
Laboratory of Advanced Materials, Fudan University
Shanghai 200438 (China)
E-mail: penghs@fudan.edu.cn

[**] This work was supported by the NSFC (grant numbers 91027025 and 21225417), MOST (grant numbers 2011CB932503 and 2011DFA51330), STCSM (grant numbers 11520701400 and 12nm0503200), Fok Ying Tong Education Foundation, and the Program for Prof. of Special Appointment at Shanghai Institutions of Higher Learning.

Supporting information for this article is available on the WWW under http://dx.doi.org/10.1002/anie.201303216.

CNTs have been widely used as energy materials because of their remarkable mechanical and electronic properties.[9–12] Generally, they are prepared in forms of powders or films in which CNTs randomly aggregate into networks. However, the network structure produces a lot of boundaries which are unfavorable for the charge separation and transport. Here aligned CNT fibers have been spun from CNT arrays based on a dry spinning process. CNT arrays were synthesized by a chemical vapor deposition process,[11,12] and they showed appropriately 200 μm in thickness. A continuous CNT fiber with a length of up to hundreds of meters could be produced from such an array, and the diameter of the CNT fiber was controlled from 6 to 40 μm by varying the width of the CNT bundle that was pulled out of the array. Figure 2a shows

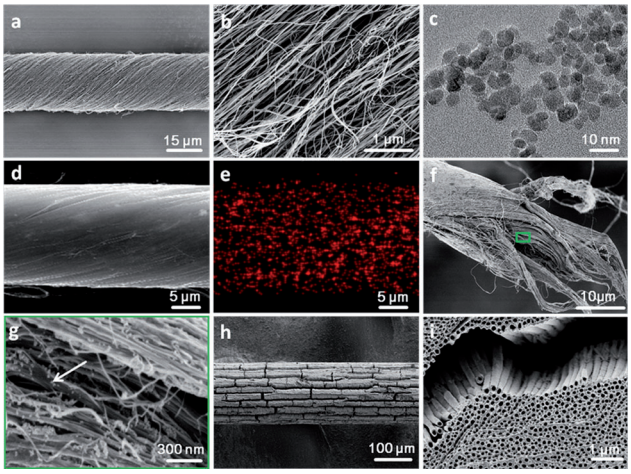

Figure 2. Characterization of a Fe_3O_4/CNT composite fiber and a TiO_2-modified Ti wire. a,b) Scanning electron microscopy (SEM) images of a bare CNT fiber at low and high magnifications, respectively. c) Transmission electron microscopy (TEM) image of Fe_3O_4 nanoparticles. d,e) SEM image and Fe mapping image of a Fe_3O_4/CNT composite fiber, respectively. f) SEM images of a broken Fe_3O_4/CNT composite fiber. g) Higher magnification of the green rectangle area in (f). The arrow shows the superparamagnetic nanoparticle. h,i) SEM images of highly aligned TiO_2 nanotubes which were grown on the surface of a titanium wire at low and high magnifications, respectively.

a typical scanning electron microscopy (SEM) image of a CNT fiber with a uniform diameter of 25 μm. As the building CNTs are highly aligned (Figure 2b), the resulting fiber exhibited excellent physical properties, for example, a light weight with a density of 0.54 $g\,cm^{-3}$, tensile strength of up to 600 MPa, and electrical conductivity on the order of 10^2–10^3 $S\,cm^{-1}$. The CNT fiber was also highly flexible and did not break under bending for more than a hundred cycles.

Two representative superparamagnetic systems, that is, Fe_3O_4 and Ni nanoparticles, were studied as two examples in this work. Fe_3O_4 nanoparticles had been most investigated for the excellent superparamagnetic property and were synthesized by a co-precipitation method.[13,14] An average diameter of 8 nm was obtained from the transmission electron microscopy observation (Figure 2c). Powder X-ray diffraction was further used to investigate the nanocrystalline structure of Fe_3O_4 nanoparticles (see Figure S1 in the Supporting Information). A cubic inverse spinel structure has been verified with characteristic peaks of (220), (311), (400), (422), (511), and (440). The Fe_3O_4 nanoparticle could be well dispersed in water. To produce composite fibers, CNT bundles close to the array were pulled through Fe_3O_4 nanoparticle dispersions (Figure S2). The Fe_3O_4 content could be easily tuned by the concentration of Fe_3O_4 nanoparticles (Figure S3). Figure 2d shows SEM image of a typical Fe_3O_4/CNT composite fiber with a uniform diameter and a smooth surface. The Fe mapping image was further used to study the structure of a composite fiber (Figure 2e), and the red dots correspond to Fe elements. Obviously, Fe_3O_4 nanoparticles are uniformly dispersed in the CNTs, which is also verified by SEM. Figure 2f and g show cross-sectional images of a breaking part in the composite fiber. Fe_3O_4 nanoparticles with a diameter of 8 nm were stably attached on the CNTs, and no obvious aggregation had been observed. Ni nanoparticles had also been studied as they are commercially available. The Ni nanoparticle with an average diameter of appropriately 20 nm was used here (Figure S4). Similar to the Fe_3O_4 nanoparticle, Ni nanoparticles could also be uniformly incorporated into the CNT fiber (Figure S5).

Aligned TiO_2 nanotubes were grown on the surface of a titanium wire by electrochemically anodizing a pure titanium wire.[12] Figure 2h shows that the modified titanium wire is uniform in diameter, that is, the TiO_2 nanotubes have the same length. Figure 2i further shows that the TiO_2 nanotubes are uniform with diameter of about 100 nm and a wall thickness of about 30 nm.

The magnetic properties of CNT composite fibers were studied by a superconducting quantum interference device at 300 K. Obviously, the synthesized composite fiber exhibit a superparamagnetic behavior confirmed by zero coercivity and remanence on the hysteresis loop (Figure 3a and Figure S6). Different saturation magnetizations were obtained for different weight percentages of Fe_3O_4 nanoparticles. High saturation magnetizations of 17.9 and 7.0 $emu\,g^{-1}$ were obtained for the composite fibers with 16.6% Fe_3O_4 and 11.2% Ni nanoparticles, respectively. The magnetic property of the composite fibers was also shown in Figure 3b and c. A composite fiber with 16.6% Fe_3O_4 nanoparticles showed a tensile strength of 600 MPa, and could hold a heavy object at the end (Figure 3c). When a magnet was approaching the fiber, it was rapidly attracted to the magnet.

A bare CNT or CNT composite fiber could be then twisted with a modified Ti wire to produce a photovoltaic wire. Because of the high flexibility, the CNT fiber could be closely and stably bundled with the Ti wire (Figure 1b and c), which is critically important for the high performance of the photovoltaic wire. As expected, the resulting photovoltaic wire could also be stably attached on a magnet. In Figure 3d and e the two devices are compared. The device on top is without Fe_3O_4 nanoparticles in the counter electrode and the device at the bottom uses Fe_3O_4 nanoparticles incorporated into the counter electrode. Obviously, only the bottom device was attracted on the magnet. Two videos had been provided for the responsive process in the Supporting Information (Videos S1 and S2).

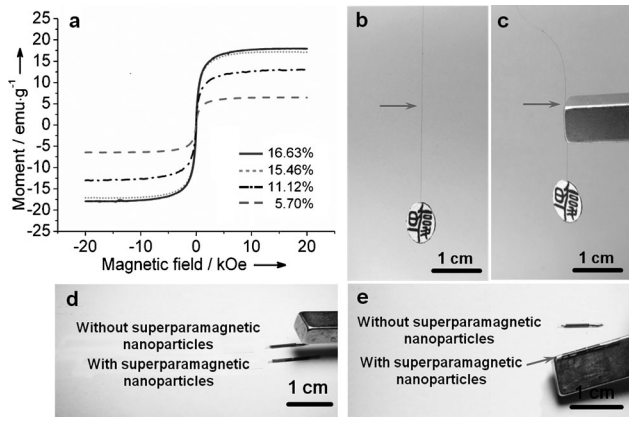

Figure 3. Magnetic responses of the superparamagnetic nanoparticle-based composite fiber and the resulting photovoltaic wire. a) Hysteresis loop of the composite fibers with different weight percentages of superparamagnetic nanoparticles. b,c) Photographs of a superparamagnetic nanoparticle/CNT composite fiber (at a diameter of about 25 μm) before and after being close to a magnet, respectively. d,e) Photographs of two photovoltaic wires before and after a magnet was moved close to them at the same distance. The top device was fabricated by twisting a bare CNT fiber and a modified titanium wire, while the bottom one was fabricated by twisting a superparamagnetic nanoparticle/CNT composite fiber and the same modified titanium wire. Here Fe_3O_4 nanoparticles with an average diameter of 8 nm had been studied.

Figure 4 shows the *J*–*V* characteristics of the photovoltaic wires using a bare CNT fiber and Ni/CNT composite fibers with an increasing amount of superparamagnetic nanoparticles as counter electrodes and a Ti wire being impregnated with aligned TiO_2 nanotubes (length of 30 μm) as the working electrode under the same condition. These photovoltaic wires were measured under AM 1.5 illumination (spectral distribution of sunlight at a zenith angle of 48.2°; AM = air mass; 100 mW cm^{-2}), and the photovoltaic parameters are compared in Table 1. Here the effective area was calculated by multiplying the length and diameter of the working electrode in the wire cell. Although the open-circuit voltage (V_{OC}) remained almost unchanged, both the short-circuit current density (J_{SC}) and the fill factor (FF) were continuously enhanced with increasing Ni weight percentage. Accordingly, the energy conversion efficiency was largely increased, for example by appropriately 20% in the case of a composite fiber with a Ni weight percentage of 11.2% compared with the bare CNT fiber.

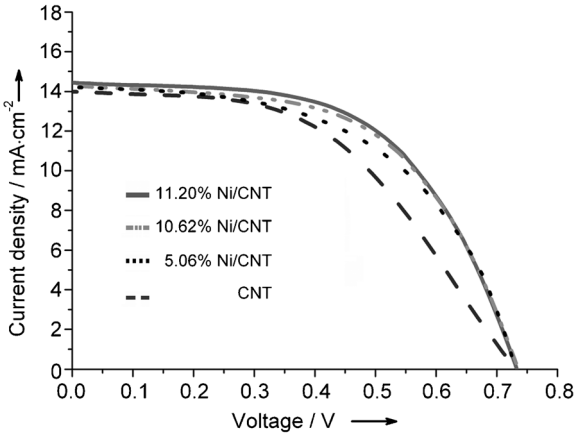

Figure 4. *J*–*V* curves of the photovoltaic wires by bare CNT fiber and Ni/CNT composite fibers as counter electrodes. Ni/CNT composite fibers with different weight percentage of Ni were used as counter electrodes. A TiO_2-modified Ti wire which was grown with TiO_2 nanotubes on the surface (length of 30 μm) had been used as the working electrode. The photovoltaic wires were measured under AM 1.5 illumination.

Table 1: Photovoltaic parameters of photovoltaic wires based on bare and composite CNT fibers with different weight percentages of Ni as counter electrodes.

Group	V_{OC} [V]	J_{SC} [mA cm^{-2}]	FF	*h* [%]
CNT	0.729	13.99	0.497	5.07
5.06% Ni/CNT	0.730	14.22	0.538	5.58
10.62% Ni/CNT	0.734	14.30	0.565	5.93
11.20% Ni/CNT	0.733	14.43	0.571	6.04

The increased efficiency can be explained by the fact that Ni nanoparticles also showed a high electrocatalytic activity.[15,16] Figure S7 shows typical cyclic voltammograms for composite fibers with increasing content of Ni nanoparticles. Two pairs of oxidation/reduction peaks have been observed in all curves, and the left corresponds to the redox reaction of I_3^-/I^-. Generally, both higher peak current density and lower peak-to-peak voltage separation correspond to a higher catalytic activity. Here the reduction peak current density was increased while the peak-to-peak voltage separation decreased with increasing Ni content of the composite fibers. On contrast, both peak current density and peak-to-peak voltage separation remained almost unchanged with an increasing content of Fe_3O_4 nanoparticles (Figure S8). The three photovoltaic parameters V_{OC}, J_{SC}, and FF of the resulting photovoltaic wires had also been maintained, and the energy conversion efficiencies were similar (Figure S9 and Table S1).

To further improve the catalytic activity and the cell performance, platinum (Pt) nanoparticles were further electrodeposited onto the superparamagnetic nanoparticle/CNT composite fiber by a double potential step electrochemical method.[17] The Pt weight percentage could be controlled between 3.85 and 44.6%, and Figure S10 shows a typical SEM image of Pt nanoparticles with an average diameter of appropriately 30 nm coated on the surface of the composite fiber. Figures S11–13 have compared cyclic voltammograms of the Pt nanoparticle-deposited superparamagnetic nanoparticle/CNT composite fibers and a Pt wire. Obviously, the Pt deposition favored a higher electrocatalytic activity than both a bare Pt wire and superparamagnetic nanoparticle/CNT composite fibers. As expected, the resulting photovoltaic wire with the Pt deposition exhibited a record efficiency of 8.03% (Figures S14 and S15).[8,18] For comparison, a Pt wire had also been used as the counter electrode to fabricate the photovoltaic wire under the same condition, and an efficiency of 6.52% was produced (Figure S16). To verify the obtained J_{sc} in these wire cells, the incident photon-to-electron conversion

efficiency was measured as a function of the wavelength (Figure S17). A high maximum value of 83% was typically obtained at a wavelength of 550 nm.

Superparamagnetic nanoparticles were introduced into the photovoltaic wire during the fabrication. If such nanoparticles were directly attached to the outer surface of the photovoltaic wire by a solution process after it had been fabricated, the cell structure would be destroyed. In addition, the nanoparticles would be peeled off under bending during the use. Furthermore, the attached nanoparticle layer would reflect the incident light, and lower energy conversion efficiencies of the photovoltaic wires were produced. Therefore, it is critically important to incorporate Fe_3O_4 nanoparticles into the fiber electrode at the beginning step of the synthesis.

The photovoltaic wire could be further extended to store the produced electric energy by integrating a supercapacitor with a high performance (Figure S18). The storage efficiency was calculated to be about 62.9%, and the total photoelectric conversion and storage efficiency can be then obtained by multiplying the photoelectric conversion efficiency and storage efficiency, which was appropriately 4.7% (Figure S19). The calculation processes are detailed in the Supporting Information.

In conclusion, this work has developed novel photovoltaic wires which could be repeatedly attached onto and detached from substrates like a post-it paper by incorporation of superparamagnetic nanoparticles. The reversible operations are remotely controlled by magnetic fields. The introduction of the superparamagnetic nanoparticle has also greatly improved the performance of photovoltaic wires. To the best of our knowledge, they have exhibited a record energy conversion efficiency of 8.03% in wire-shaped devices. The combined advantages are promising to the portable and wearable electronic applications. This work also provides a fabrication method for the development of new energy devices.

Experimental Section

The synthetic details of CNT arrays and Fe_3O_4 nanoparticles are described in the Supporting Information. Fe_3O_4/CNT and Ni/CNT composite fibers were then prepared by a dry spinning process. A spinnable CNT array was first fixed on a clean substrate. To produce composite fibers, CNT bundles were pulled out of the array and through the superparamagnetic nanoparticle dispersion (Figure S2). Composite fibers with different Fe_3O_4 and Ni contents were controlled by varying the concentrations of their dispersions in water, respectively. The fibers were dried in vacuum prior to the fabrication of photovoltaic wires. Pt nanoparticles were electrodeposited onto CNT composite fibers by a double potential step method in a conventional glass container at room temperature. The electrolyte was composed of 1 mM K_2PtCl_6 and 0.1M KCl in water. A platinum wire and a Ag/AgCl/KCl electrode were used as counter and reference electrodes with the first step at E1 of 0.5 V for 10 s and the second step at E2 of −0.7 V for 10 s, respectively. The resulting fibers were then washed with deionized water and dried in vacuum prior to use. Aligned TiO_2 nanaotube arrays were grown on the surface of a Ti wire by an electrochemical anodization in 0.3 wt% NH_4F/ethylene glycol solution containing 8 wt% H_2O at voltages of 60 V for 6 h. The anodization was performed in a two-electrode electrochemical cell with the Ti wire (diameter of 127 μm and purity of 99.9%) and Pt sheet as anode and cathode, respectively. The resulting wires were washed with deionized water twice to remove the electrolyte, followed by heating to 500°C for 1 h and annealing in air.

To fabricate the photovoltaic wire, the modified Ti wire was first immersed in a 40 mM $TiCl_4$ aqueous solution at 70°C for 30 minutes, and then rinsed with deionized water, followed by annealing again at 450°C for 30 minutes. After the temperature was decreased to 120°C, it was immersed into 0.3 mM N719 solution in a mixture solvent of dehydrated acetonitrile and tert-butanol (volume ratio of 1/1) for 16 h. Finally, the dye-absorbed working electrode was twisted with a CNT fiber, Fe_3O_4/CNT fiber or Pt/Fe_3O_4/CNT fiber as counter electrode to form a wire cell which can be sealed in a capillary glass tube or transparent flexible fluorinated ethylene propylene tube. Two electrodes were extracted and modified by indium. The redox electrolyte (containing 0.1M lithium iodide, 0.05M iodine, 0.6M 1,2-dimethyl-3-propylimidazolium iodide, and 0.5M 4-tert butyl-pyridine in dehydrated acetonitrile) was introduced to the cell prior to the characterization.

Received: April 17, 2013
Published online: June 26, 2013

Keywords: carbon nanotubes · fibers · magnetic properties · nanoparticles · photovoltaic wires

[1] a) T. Miyasaka, T. N. Murakami, *Appl. Phys. Lett.* **2004**, *85*, 3932–3934; b) H. W. Chen, C. Y. Hsu, J. G. Chen, K. M. Lee, C. C. Wang, K. C. Huang, K. C. Ho, *J. Power Sources* **2010**, *195*, 6225–6231.

[2] G. Wee, T. Salim, Y. M. Lam, S. G. Mhaisalkar, M. Srinivasan, *Energy Environ. Sci.* **2011**, *4*, 413–416.

[3] Z. B. Yang, L. Li, Y. Luo, R. He, L. Qiu, H. Lin, H. S. Peng, *J. Mater. Chem. A* **2013**, *1*, 954–958.

[4] Y. Xue, J. Liu, H. Chen, R. Wang, D. Li, J. Qu, L. Dai, *Angew. Chem.* **2012**, *124*, 12290–12293; *Angew. Chem. Int. Ed.* **2012**, *51*, 12124–12127.

[5] a) A. W. Hains, Z. Liang, M. A. Woodhouse, B. A. Gregg, *Chem. Rev.* **2010**, *110*, 6689–6735; b) S. Huang, L. Li, Z. Yang, Zhang, L. H. Saiyin, T. Chen, H. Peng, *Adv. Mater.* **2011**, *23*, 4707–4710; c) Z. Yang, T. Chen, R. He, H. Li, H. Lin, L. Li, G. Zou, Q. Jia, H. Peng, *Polym. Chem.* **2013**, *1*, 1680–1684; d) T. Chen, L. Qiu, Z. Yang, H. Peng, *Chem. Soc. Rev.* **2013**, *42*, 5031–5041.

[6] Z. Wang, W. Wu, *Angew. Chem.* **2012**, *124*, 11868–11891; *Angew. Chem. Int. Ed.* **2012**, *51*, 11700–11721.

[7] a) B. Wang, J. Hai, Z. Liu, Q. Wang, Z. Yang, S. Sun, *Angew. Chem.* **2010**, *122*, 4680–4683; *Angew. Chem. Int. Ed.* **2010**, *49*, 4576–4579.

[8] a) T. Chen, S. Wang, Z. Yang, Q. Feng, X. Sun, L. Li, Z. Wang, H. Peng, *Angew. Chem.* **2011**, *123*, 1855–1859; *Angew. Chem. Int. Ed.* **2011**, *50*, 1815–1819; b) T. Chen, L. Qiu, H. Li, H. Peng, *J. Mater. Chem.* **2012**, *22*, 23655–23658; c) T. Chen, L. Qiu, H. G. Kia, Z. Yang, H. Peng, *Adv. Mater.* **2012**, *24*, 4623; d) T. Chen, L. Qiu, Z. Cai, F. Gong, Z. Yang, Z. Wang, H. Peng, *Nano Lett.* **2012**, *12*, 2568; e) S. Zhang, C. Y. Ji, Z. Q. Bian, R. H. Liu, X. Y. Xia, D. Q. Yun, L. H. Zhang, C. H. Huang, A. Y. Cao, *Nano Lett.* **2011**, *11*, 3383–3387.

[9] Z. Chen, V. Augustyn, J. Wen, Y. W. Zhang, M. Q. Shen, B. Dunn, Y. F. Lu, *Adv. Mater.* **2011**, *23*, 791–795.

[10] K. P. Gong, S. Chakrabarti, L. M. Dai, *Angew. Chem.* **2008**, *120*, 5526–5530; *Angew. Chem. Int. Ed.* **2008**, *47*, 5446–5450.

[11] Z. B. Yang, T. Chen, R. X. He, G. Z. Guan, H. P. Li, L. B. Qiu, H. S. Peng, *Adv. Mater.* **2011**, *23*, 5436–5439.

[12] H. Peng, X. Sun, F. Cai, X. Chen, Y. Zhu, G. Liao, D. Chen, Q. Li, Y. Lu, Y. Zhu, Q. Jia, *Nat. Nanotechnol.* **2009**, *4*, 738–741.

[13] A. Shkilnyy, E. Munnier, K. Herve, M. Souce, R. Benoit, S. Cohen-Jonathan, P. Limelette, M. L. Saboungi, P. Dubois, I. Chourpa, *J. Phys. Chem. C* **2010**, *114*, 5850 – 5858.
[14] X. Chen, L. Li, X. Sun, Y. Liu, B. Luo, C. Wang, Y. Bao, H. Xu, H. Peng, *Angew. Chem.* **2011**, *123*, 5600 – 5603; *Angew. Chem. Int. Ed.* **2011**, *50*, 5486 – 5489.
[15] P. Joshi, Z. P. Zhou, P. Poudel, A. Thapa, X. F. Wu, Q. Q. Qiao, *Nanoscale* **2012**, *4*, 5659 – 5664.
[16] T. Ma, X. Fang, M. Akiyama, K. Inoue, H. Noma, E. Abe, *J. Electroanal. Chem.* **2004**, *547*, 77 – 83.
[17] H. F. Cui, J. S. Ye, W. D. Zhang, J. Wang, F. S. Sheu, *J. Electroanal. Chem.* **2005**, *577*, 295 – 302.
[18] Y. Fu, Z. Lv, S. Hou, H. Wu, D. Wang, C. Zhang, Z. Chu, X. Cai, X. Fan, Z. L. Wang, D. Zou, *Energy Environ. Sci.* **2011**, *4*, 3379 – 3385.

